Noticeable positive Doppler effect on optical bistability in an N-type active Raman gain atomic system*

Chang Zeng-Guang(常增光)[a)], Niu Yue-Ping(钮月萍)[b)], Zhang Jing-Tao(张敬涛)[a)], and Gong Shang-Qing(龚尚庆)[b)†]

[a)] *State Key Laboratory of High Field Laser Physics, Shanghai Institute of Optics and Fine Mechanics, Chinese Academy of Sciences, Shanghai* 201800, *China*

[b)] *Department of Physics, East China University of Science and Technology, Shanghai* 200237, *China*

(Received 1 February 2012; revised manuscript received 23 April 2012)

We theoretically investigate the Doppler effect on optical bistability in an N-type active Raman gain atomic system inside an optical ring cavity. It is shown that the Doppler effect can greatly enhance the dispersion and thus create the bistable behaviour or greatly increase the bistable region, which has been known as the positive Doppler effect on optical bistability. In addition, we find that a positive Doppler effect can change optical bistability from the hybrid dispersion-gain type to a dispersive type.

Keywords: positive Doppler effect, optical bistability, N-type atomic system, active Raman gain

PACS: 42.65.Pc, 42.50.Gy **DOI:** 10.1088/1674-1056/21/11/114210

1. Introduction

Optical bistability (OB) has caught much attention in the past few years due to its potential applications in optical switching, optical transistors, and optical storage elements, which are essential for optical computing and communications. Controlled OB via induced atomic coherence in multilevel atomic systems was investigated theoretically and experimentally.[1−14] For example, it was shown that bistable behaviour can be controlled by the initial coherence in a Λ-type atomic system.[5] Also, it was found that spontaneously generated coherence (SGC) could significantly affect OB behaviour in a three-level atomic system.[7] Controlled OB via the phase of coherent coupling fields has also been studied.[8−10] Furthermore, it has been reported that the shift of an OB hysteresis curve is dependent on the nonlinear phase shift induced by a controlling light in the four-level atomic system of ^{87}Rb inside the optical ring cavity.[11] In addition, it was found that the hybrid absorptive–dispersive OB can be controlled by adjusting the intensity and detuning the coupling field; optical multistability (OM) can also be observed under appropriate detuning in an N-type atomic medium.[13]

It was shown theoretically and experimentally that Doppler broadening can exert remarkable effects on the probe absorption and dispersion responses of three-level and four-level atomic systems.[15−18] Active Raman gain systems have also attracted a great deal of attention in the past few years.[19−23] Recently, Zhang *et al.* considered a combination of these two aspects and proposed a scheme for the extremely narrowed and amplified gain spectrum induced by the Doppler effect in an N-type active Raman gain ^{87}Rb atomic system.[24] Since the probe field was weak, the nonlinear susceptibility was negligible and could be safely neglected, then just the linear susceptibility was considered by them. However, when susceptibility is dependent on the probe intensity, the susceptibility, including liner and nonlinear susceptibilities, needs to be considered, which is the case we will study here.

In this paper, we study the effect of Doppler broadening on OB in an N-type active Raman gain ^{87}Rb atomic system. Our results show that Doppler broadening can subsequently enhance the dispersion and produce a remarkable positive effect on OB near the double photon resonance. Furthermore, it is found that Doppler broadening can change hybrid dispersion-gain OB to a dispersive one.

*Project supported by the National Natural Science Foundation of China (Grant No. 60978013) and the Shanghai Rising Star Project, China (Grant No. 11QA1407400).

†Corresponding author. E-mail: sqgong@siom.ac.cn

© 2012 Chinese Physical Society and IOP Publishing Ltd

2. Model and method

As mentioned above, we consider an N-type four-level scheme. The relevant atomic levels in ^{87}Rb are plotted in Fig. 1, $5S_{1/2}$, $F = 1$, 2 of ^{87}Rb are chosen to be $|1\rangle$ and $|3\rangle$, respectively, $5P_{1/2}$, $F = 1$ to be $|2\rangle$, and $5P_{3/2}$, $F = 2$ to be $|4\rangle$. A driving field with amplitude $E_{\rm d}$ and angular frequency $\omega_{\rm d}$ is applied to drive the transition $|1\rangle \leftrightarrow |2\rangle$ of frequency ω_{12}. A probe field with amplitude $E_{\rm p}$ and angular frequency $\omega_{\rm p}$ is applied to drive the transition $|2\rangle \leftrightarrow |3\rangle$ of frequency ω_{23}. The transition $|3\rangle \leftrightarrow |4\rangle$ of frequency ω_{34} is driven by a control field with amplitude $E_{\rm c}$ and angular frequency $\omega_{\rm c}$, which is applied to control the Raman gain process. The driving and probe fields are assumed to be far-detuned from the corresponding transitions, while the control field is assumed to be near-resonant with the corresponding transition. In the interaction picture with the rotating-wave approximation, the semiclassical Hamiltonian of the system under study can be expressed as (taking $\hbar = 1$)[24]

$$\begin{aligned} H_{\rm int} =& -\Delta_{\rm d}|2\rangle\langle 2| - (\Delta_{\rm d} - \Delta_{\rm p})|3\rangle\langle 3| \\ & - (\Delta_{\rm d} + \Delta_{\rm c} - \Delta_{\rm p})|4\rangle\langle 4| \\ & - (\Omega_{\rm d}|2\rangle\langle 1| + \Omega_{\rm p}|2\rangle\langle 3| + \Omega_{\rm c}|4\rangle\langle 3| + {\rm H.c.}), \end{aligned} \tag{1}$$

where Ω_n ($n = {\rm d}, {\rm p}, {\rm c}$) stands for half of the Rabi frequency of the corresponding transition, i.e., $\Omega_{\rm d} = \mu_{21}E_{\rm d}/2\hbar$, $\Omega_{\rm p} = \mu_{23}E_{\rm p}/2\hbar$, and $\Omega_{\rm c} = \mu_{43}E_{\rm c}/2\hbar$. Here, $\mu_{ij} = \boldsymbol{\mu}_{ij} \cdot \hat{\boldsymbol{e}}_L$ ($\hat{\boldsymbol{e}}_L$ is the polarization unit vector of the laser field) denotes the dipole moment for the transition between levels $|i\rangle$ and $|j\rangle$, $\Delta_{\rm d} = \omega_{\rm d} - \omega_{21}$, $\Delta_{\rm p} = \omega_{\rm p} - \omega_{23}$, and $\Delta_{\rm c} = \omega_{\rm c} - \omega_{43}$ are the detunings of the driving, the probe, and the control fields for the corresponding transitions (see Fig. 1). Taking into account spontaneous emissions and decoherences, we can write the density-matrix equations of motion as

$$\begin{aligned} \dot{\rho}_{11} =& \gamma_{21}\rho_{22} + \gamma_{41}\rho_{44} + {\rm i}\Omega_{\rm d}(\rho_{21} - \rho_{12}), \\ \dot{\rho}_{22} =& -(\gamma_{21} + \gamma_{23})\rho_{22} + {\rm i}\Omega_{\rm d}(\rho_{12} - \rho_{21}) \\ & + {\rm i}\Omega_{\rm p}(\rho_{32} - \rho_{23}), \\ \dot{\rho}_{33} =& \gamma_{23}\rho_{22} + \gamma_{43}\rho_{44} + {\rm i}\Omega_{\rm p}(\rho_{23} - \rho_{32}) \\ & + {\rm i}\Omega_{\rm c}(\rho_{43} - \rho_{34}), \\ \dot{\rho}_{44} =& -(\gamma_{41} + \gamma_{43})\rho_{44} + {\rm i}\Omega_{\rm c}(\rho_{34} - \rho_{43}), \\ \dot{\rho}_{21} =& [-(\gamma_{21} + \gamma_{23})/2 - {\rm i}\Delta_{\rm d}]\rho_{21} \\ & + {\rm i}\Omega_{\rm d}(\rho_{11} - \rho_{22}) + {\rm i}\Omega_{\rm p}\rho_{31}, \\ \dot{\rho}_{31} =& -{\rm i}(\Delta_{\rm d} - \Delta_{\rm p})\rho_{31} + {\rm i}(\Omega_{\rm p}\rho_{21} + \Omega_{\rm c}\rho_{41} - \Omega_{\rm d}\rho_{32}), \\ \dot{\rho}_{41} =& [-(\gamma_{41} + \gamma_{43})/2 - {\rm i}(\Delta_{\rm d} - \Delta_{\rm p} + \Delta_{\rm c})]\rho_{41} \\ & + {\rm i}(\Omega_{\rm c}\rho_{31} - \Omega_{\rm d}\rho_{42}), \\ \dot{\rho}_{32} =& [-(\gamma_{21} + \gamma_{23})/2 + {\rm i}\Delta_{\rm p}]\rho_{32} + {\rm i}\Omega_{\rm p}(\rho_{22} - \rho_{33}) \\ & + {\rm i}(\Omega_{\rm c}\rho_{42} - \Omega_{\rm d}\rho_{31}), \\ \dot{\rho}_{42} =& [-(\gamma_{21} + \gamma_{23} + \gamma_{41} + \gamma_{43})/2 - {\rm i}(\Delta_{\rm c} - \Delta_{\rm p})]\rho_{42} \\ & + {\rm i}(\Omega_{\rm c}\rho_{32} - \Omega_{\rm d}\rho_{41} - \Omega_{\rm p}\rho_{43}), \\ \dot{\rho}_{43} =& [-(\gamma_{41} + \gamma_{43})/2 - {\rm i}\Delta_{\rm c}]\rho_{43} \\ & + {\rm i}\Omega_{\rm c}(\rho_{33} - \rho_{44}) - {\rm i}\Omega_{\rm p}\rho_{42}, \end{aligned} \tag{2}$$

with $\rho_{kj}^* = \rho_{jk}$. The decay rates from excited states $|2\rangle$ and $|4\rangle$ to ground states $|1\rangle$ and $|3\rangle$ are γ_{21}, γ_{23}, γ_{41}, and γ_{43}, respectively. The relaxation rates of coherence between ground states $|1\rangle$ and $|3\rangle$ are negligible and will be neglected. Raman detunings have $\Delta_{\rm d}$, $\Delta_{\rm p} \gg \Delta_{\rm c}$, $\Omega_{\rm d}$, $\Omega_{\rm p}$, $\Omega_{\rm c}$, γ_{21}, γ_{23}, γ_{41}, γ_{43}. All laser fields are assumed to copropagate in the atomic medium. In the case of thermal atomic vapor, the effects of the Doppler broadening should be included in Eq. (2), and $\Delta_{\rm d}, \Delta_{\rm p}$, and $\Delta_{\rm c}$ need to be replaced by $\Delta_{\rm d} + k_{\rm d}v, \Delta_{\rm p} + k_{\rm p}v$, and $\Delta_{\rm c} + k_{\rm c}v$, where $k_n = \omega_n/c$ ($n = {\rm d}, {\rm p}, {\rm c}$) is the wave vector of the corresponding laser field, and v is the projection of the atomic velocity along the laser beams.

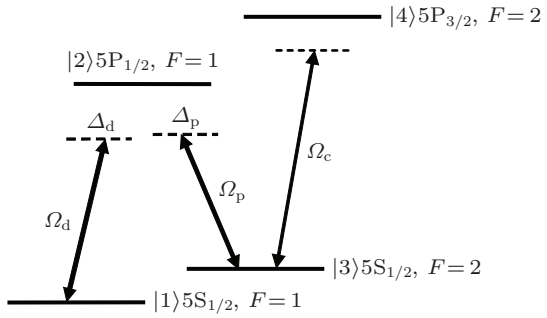


Fig. 1. Schematic diagram of a ^{87}Rb atom interacting with a driving field with Rabi frequency $2\Omega_{\rm d}$, a probe field with Rabi frequency $2\Omega_{\rm p}$, and a control field with Rabi frequency $2\Omega_{\rm c}$. The ground state hyperfine levels $5S_{1/2}$, $F = 1$, 2 of ^{87}Rb are chosen to be $|1\rangle$ and $|3\rangle$, respectively, $5P_{1/2}$, $F = 1$ to be $|2\rangle$, and $5P_{3/2}$, $F = 2$ to be $|4\rangle$.

The atomic medium is put in an unidirectional ring cavity, as shown in Fig. 2; note that only the probe field $E_{\rm p}$ circulates in the ring cavity. For simplicity, we assume that mirrors 3 and 4 have 100% reflection, while mirrors 1 and 2 have the intensity reflection and transmission coefficients of $R_{\rm c}$ and $T_{\rm c}$ ($R_{\rm c}+T_{\rm c} = 1$). The dynamic response of the probe field is governed by Maxwell's equation under the slowly

varying envelope approximation

$$\frac{\partial E_{\rm p}}{\partial t}+c\frac{\partial E_{\rm p}}{\partial z}=\mathrm{i}\frac{\omega_{\rm p}}{2\varepsilon_0}P(\omega_{\rm p},T), \tag{3}$$

where c and ε_0 are the light speed and the permittivity of the free space, respectively. The $P(\omega_{\rm p},T)$ is the slowly oscillating term of the induced polarization in transition $|2\rangle\leftrightarrow|3\rangle$ at the medium temperature T, and is given by

$$P(\omega_{\rm p},T)=\mu_{23}\int_{-\infty}^{\infty}N(v,T)\rho_{23}(\omega_{\rm p},v)\mathrm{d}v, \tag{4}$$

where $N(v,T)=N_0\,\mathrm{e}^{-v^2/v_{\rm p}^2}/(\sqrt{\pi}v_{\rm p})$ is the Maxwell velocity distribution, N_0 stands for the number density of the atoms, $v_{\rm p}=\sqrt{2k_{\rm B}T/m}$ denotes the most probable velocity of the atoms, and $k_{\rm B}$ and m are the Boltzmann constant and the atomic mass, respectively.

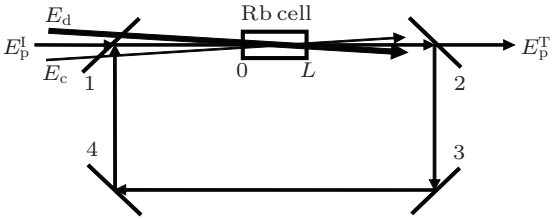


Fig. 2. Unidirectional ring cavity with an atomic sample of length L containing N inhomogeneously broadened atoms with their atomic configuration given in Fig. 1. Here $E_{\rm p}^{\rm I}$ and $E_{\rm p}^{\rm T}$ are the incident and transmitted fields, and $E_{\rm d}$ and $E_{\rm c}$ are the driving and control fields, respectively. For mirrors 1 and 2, $R_{\rm c}+T_{\rm c}=1$, and mirrors 3 and 4 have $R_{\rm c}=1$.

For a perfectly tuned ring cavity, the boundary conditions in the steady-state are

$$\begin{aligned}&E_{\rm p}(L)=E_{\rm p}^{\rm T}/\sqrt{T_{\rm c}},\\&E_{\rm p}(0)=\sqrt{T_{\rm c}}E_{\rm p}^{\rm I}+R_{\rm c}E_{\rm p}(L),\end{aligned} \tag{5}$$

where $E_{\rm p}^{\rm I}$ and $E_{\rm p}^{\rm T}$ are the incident and the transmitted fields, respectively, and L is the length of the atomic sample. The second term on the right-hand side of Eq. (5) describes a feedback mechanism relevant to the mirrors, which is essential to give rise to the bistability, namely, there will be no bistability if $R_{\rm c}=0$.

We can obtain the input–output relationship by using the boundary condition Eq. (5) in the mean-field limit as

$$y=x-\mathrm{i}C\gamma_{23}\int_{-\infty}^{\infty}\mathrm{e}^{-v^2/v_{\rm p}^2}/(\sqrt{\pi}v_{\rm p})\rho_{23}\mathrm{d}v, \tag{6}$$

where $y=\mu_{23}E_{\rm p}^{\rm I}/\hbar\sqrt{T_{\rm c}}$ and $x=\mu_{23}E_{\rm p}^{\rm T}/\hbar\sqrt{T_{\rm c}}$ are the normalized incident and output fields, respectively, and $C=LN_0\omega_{\rm p}\mu_{23}^2/2\hbar c\varepsilon_0T_{\rm c}\gamma_{23}$ is the usual cooperation parameter. Without loss of generality, we assume that all Rabi frequencies are real. We could assume $\gamma_{21}=\gamma_{23}=\gamma_{41}=\gamma_{43}=\gamma=2\pi\times3$ MHz and $k_{\rm d}=k_{\rm c}=k_{\rm p}=\omega_{\rm p}/c$ for simplicity, since these decay rates and also the transition frequencies of the related states are approximately equal.

3. Numerical results and discussion

First, we show the behaviours of the output–input fields in the cold and room-temperature media respectively. Setting all the time derivatives in Eq. (2) to zero for the steady state, we can obain an exact analytical expression for ρ_{23} via simple Mathematica codes. Because the analytical expression for ρ_{23} is severely tedious, we do not present it here. All the parameters are scaled with γ in the following numerical calculations. The drive field Rabi frequency is $\Omega_{\rm d}=3$, and the driving field detuning is $\Delta_{\rm d}=300$. The control field Rabi frequency is $\Omega_{\rm d}=1$, and the control field is tuned into resonance with the transition $|3\rangle\leftrightarrow|4\rangle$. These values remain fixed in all of our analyses. The probe field detuning needs to be chosen carefully, we will understand this point in the following. We choose the probe detuning $\Delta_{\rm d}=299.16$ and 298.66 respectively. To obtain distinct bistable behaviours, we choose a large cooperation parameter, i.e., C=1800, which may be realized by increasing the atomic density N_0 appropriately. We plot the input intensity versus the output intensity in Figs. 3(a) and 3(b) using Eq. (6). It is obvious that if $\Delta_{\rm p}=299.16$, almost no bistable behaviour occurs in the cold atomic medium (Fig. 3(a)). However, when the Doppler effect is considered at room temperature, noticeable bistable behaviour arises in the medium (Fig. 3(a)). In other words, the Doppler effect can create bistable behaviour in the room-temperature medium. If $\Delta_{\rm p}=298.66$, bistable behaviour occurs with a small bistable region in the cold medium, while bistable behaviour appears with a large bistable region in the medium at room temperature (Fig. 3(b)). Therefore, the Doppler effect can also greatly increase the bistable threshold if the probe detuning is decreased slightly. In both cases, we can clearly see the noticeable positive Doppler effect on OB.

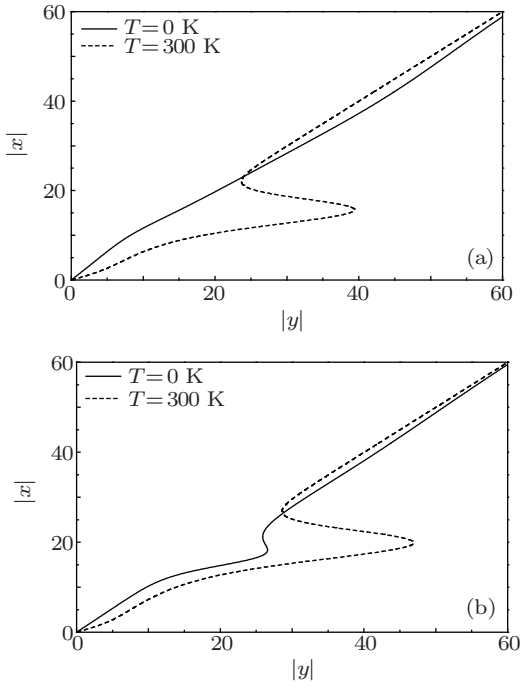


Fig. 3. The output intensity $|x|$ versus the input intensity $|y|$ in the cold and room-temperature media, where in panel (a) $\Delta_{\rm p} = 299.16$, and in panel (b) $\Delta_{\rm p} = 298.66$. The other parameters are $\Omega_{\rm d} = 3$, $\Omega_{\rm c} = 1$, $\Delta_{\rm d} = 300$, $\Delta_{\rm c} = 0$, and $C = 1800$.

The physical mechanism of such an unexpected effect can be understood in the following way. First, we examine the effect of atomic velocity on the probe gain and dispersion spectra. The probe gain and dispersion for the moving atoms at various velocities can be calculated by using the analytical expression for ρ_{23}, which is dependent on v. We choose a large probe field intensity, i.e., $\Omega_{\rm p} = 15$, with which the dispersion and gain properties can be understood better when the bistable threshold appears. Figures 4(a) and 4(b) show that if the velocity of the atom increases, the corresponding probe gain diminishes dramatically, while the corresponding dispersion is enhanced substantially near the double-photon resonance. This phenomenon can be understood as follows. For the moving atom, the control field detuning is $k_{\rm c}v$. Compared with the cold medium in which the control field is resonant with the corresponding transition, in the room-temperature medium, the control field detuning decreases the population transfer from level $|3\rangle$ to level $|4\rangle$, which results in a decline of the population decay from level $|4\rangle$ to level $|2\rangle$. This means that the probe gain is suppressed. Along with the suppressed gain, probe dispersion is enhanced due to the control field detuning.[24] Furthermore, we calculate probe gain and dispersion versus probe detuning for the cold and room-temperature media respectively. For the cold medium, we use the analytical expression for ρ_{23} without v. For the room-temperature medium, we need to calculate ρ_{23} with an integration over the Maxwell velocity distribution, i.e., the Doppler average. Figure 5 indicates that in the cold atomic system, although the dispersion is significantly stronger than the gain near the double-photon resonance, the gain can still make an appreciable contribution to the bistable threshold. According to Eq. (6), the probe gain will make the bistable value diminish. So, in this case, bistable behaviour is determined by the nonlinear behaviour of the dispersion and gain. Therefore, the bistable behaviour in the cold atomic system can be considered as the hybrid dispersion-gain type. However, for the medium at room temperature, the Doppler average enhances the dispersion and suppresses the gain dramatically. At $\Delta_{\rm p} = 299.16$ and 298.66, the dispersions in the room-temperature medium are 5 times and 1.4 times of those in the cold medium, respectively, while the corresponding gains become vanishingly small. In this case, the bistable behaviour is determined by the nonlinear behaviour of the enhanced dispersion. This is to say that the enhanced dispersion results in a great enhancement of the bistable threshold. At the same time, the OB is changed from the hybrid dispersion-gain type to the dispersive type.

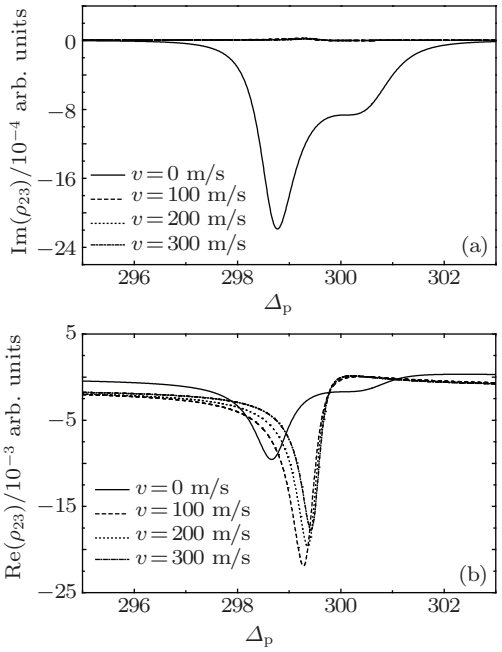


Fig. 4. The effects of atomic velocity on (a) the probe gain and (b) the probe dispersion each as a function of the probe detuning, where $\Omega_{\rm p} = 15$, the other parameters are the same as those in Fig. 3.

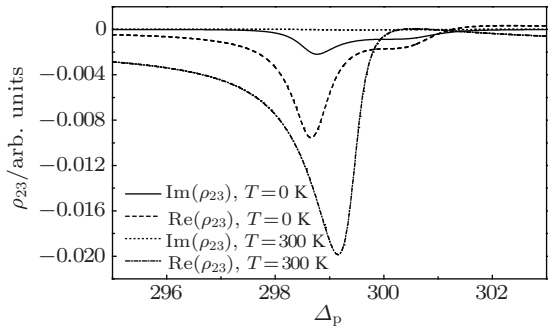


Fig. 5. (colour online) The probe gain and dispersion versus the probe detuning in the cold and room-temperature media. The parameters are the same as those in Fig. 4.

4. Conclusion

In conclusion, we study the positive Doppler effect on OB in a room-temperature N-type active Raman gain atomic system inside an optical ring cavity. On one hand, the Doppler effect can produce OB or noticeably broaden the OB region. On the other hand, the Doppler effect may change the OB from the hybrid dispersion-gain type to the dispersive type completely. The analysis shows that the Doppler effect could lead to enhanced dispersion, which may cause an increase in the bistable region. Our results may provide a clue to achieve a noticeable bistable behaviour in a room-temperature atomic system, which may have potential applications in devising optical elements.

References

[1] Abraham E and Hassan S S 1980 *Opt. Commun.* **35** 291
[2] Harshawardhan W and Agarwal G S 1996 *Phys. Rev.* A **53** 1812
[3] Wang H, Goorskey D J and Xiao M 2001 *Phys. Rev.* A **65** 011801(R)
[4] Gong S Q, Du S D, Xu Z Z and Pan S H 1996 *Phys. Lett.* A **222** 237
[5] Gong S Q, Du S D and Xu Z Z 1997 *Phys. Lett.* A **226** 293
[6] Chen Z Y, Zhang J T and Xu Z Z 1999 *Chin. Phys.* B **8** 902
[7] Joshi A, Yang W G and Xiao M 2003 *Phys. Lett.* A **315** 203
[8] Cheng D C, Liu C P and Gong S Q 2006 *Opt. Commun.* **263** 111
[9] Wang Z P and Fan H Y 2010 *Journal of Luminescence* **130** 2084
[10] Xiao Z H and Kim K 2010 *Opt. Commun.* **283** 2178
[11] Chang H, Wu H B, Xie C D and Wan H 2004 *Phys. Rev. Lett.* **93** 213901
[12] Chen A X, Wang Z P, Chen D H and Xu Y Q 2009 *Chin. Phys.* B **18** 1072
[13] Li J H, Lü X Y, Luo J M and Huang Q J 2006 *Phys. Rev.* A **74** 035801
[14] Mahmoudi M, Mousavi S M and Sahrai M 2010 *Eur. Phys. J.* D **57** 241
[15] Kong L B, Tu X H, Wang J, Zhu Y F and Zhan M S 2007 *Opt. Commun.* **269** 362
[16] Iftiquar S M, Karve G R and Natarajan V 2008 *Phys. Rev.* A **77** 063807
[17] Bason M G, Mohapatra A K, Weatherill K J and Adams C S 2009 *J. Phys.* B: *At. Mol. Opt. Phys.* **42** 075503
[18] Jia K N, Liang Y, Liu Z B, Tong D M and Fan X J 2012 *Acta. Phys. Sin.* **61** 54207 (in Chinese)
[19] Agarwal G S and Dasgupta S 2004 *Phys. Rev.* A **70** 023802
[20] Jiang K J, Deng L and Payne M G 2006 *Phys. Rev.* A **74** 041803
[21] Huang G X, Hang C and Deng L 2008 *Phys. Rev.* A **77** 011803(R)
[22] Hang C and Huang G X 2010 *Opt. Express* **18** 2952
[23] Li H J, Dong L W, Hang C and Huang G X 2011 *Phys. Rev.* A **83** 023816
[24] Zhang L D, Jiang Y, Wan R G, Tian S C, Zhang B, Zhang X J, Gao J Y, Niu Y P and Gong S Q 2011 *J. Phys.* B *At. Mol. Opt. Phys.* **44** 135505